OPTICAL CHARACTERIZATION OF AS-DEPOSITED AND AIR-ANNEALED CdS FILM GROWN BY CBD TECHNIQUE

Z. RIZWAN[a], N. KAMILAH SA'AT[b], A. ZAKARIA[b*]
[a]*National Textile University, Sheikhupur Road, 37610 Faisalabad, Pakistan*
[b]*Department of Physics, Faculty of Science, University Putra Malaysia, 43400 Serdang, Selangor D.E., Malaysia*

CdS thin films were deposited on commercial glass substrate using CBD technique from bath with low solution concentrations of cadmium chloride and thiourea. The film adhesion was excellent for all samples. The films samples were air annealed at 200 ^{o}C for 60 minutes. The observed minimum film thickness was 34.8 nm. XRD analyses results show that the film samples were cubic CdS in as-deposited film samples. Very feeble peaks of hexagonal phase were observed in all air-annealed samples except the samples at higher solution concentration. Crystallite size was increased from 27.2, 19.8 to 52.6, 70 nm with the increase of cadmium chloride and thiourea concentration for thin film samples as-deposited and annealed samples, respectively. E_g, E_{oo} and α was determined from the transmittance data. The best transmittance (> 96 %) was obtained for longer wavelength range in this experiment.

(Received April 1, 2017;Accepted October 10, 2017)

Keywords: CBD, CdS, Optical properties, air-annealing

1. Introduction

Several techniques are being used to grow thin films e.g., sputtering, electro-deposition, vacuum evaporation MBE, MOCVD, CSS, pulsed laser evaporation, radio frequency, SILAR, SPD and chemical bath deposition (CBD). CBD technique has an attractive due to its simplicity, low deposition temperature, large area deposition and low cost. CBD technique also has tremendous control to grow thin films uniformly [1]. This technique increases the efficiency CdS window layer. Maximum efficiency was also achieved when this technique was used to develop buffer layer for CdTe, CIGS and photovoltic cells [2-5]. This popular technique is also used in the fabrication of sophisticated electronic [6-7]. Cadmium sulfide is an admirable hetrojunction partner for the p-type $CuInSe_2$, CdTe, $Cu(In,Ga)Se_2$ due to the wide energy band gap that is 2.42 eV. It is also significant because of its unique properties for example, high refractive index having the value 2.5, photoconductivity and higher electron affinity [8-11]. The substrate was dipped in aqueous solution having alkaline nature in chemical bath which contains S^{2-} and Cd^{2+} ions produced by the chemical reaction in solution [12, 13]. pH of aqueous solution, temperature, time for thin film deposition, relative concentrations of reactive which provide ions for the chemical reaction are main parameters to control growth rate of film.

This excellent CBD technique has been carried out to grow CdS films on commercial glass slides with the solution concentrations of cadmium chloride [0.000625 - 0.005 M] and thiourea [0.00125 - 0.01 M] in this study. The structural and optical properties of CdS thin films as-deposited and air-annealed have been discussed with the increased solution concentrations.

*Corresponding author: azmizak@upm.edu.my

2. Experimental

$CdCl_2$ [Alfa Aeser, 4N purity,] and [$(NH_2)_2CS$ (Alfa Aeser, 3N purity] were used to grow CdS thin films on microscopic commercial glass slides as substrate. Substrates were immersed in 4% HCl for cleaning and the further cleaned with acetone and methanol, ultrasonically.

All calculations in this experiment are molar solution concentrations. About 55 ml aqueous solution of $CdCl_2$ [0.00312, 0.000625, 0.00125, 0.0025 and 0.005] and $(NH_2)_2CS$ [0.000625, 0.00125, 0.0025, 0.005 and 0.01] were prepared in a glass beaker in doubly deionized H_2O to obtain the source of Cd^{2+} and S^{2-} ions, respectively under constant stirring at the room temperature. The ratio of $CdCl_2$ to $(NH_2)_2CS$ = has been kept constant as 1:2 as in our previous papers [14, 15]. The beaker of the solution of $CdCl_2$ was placed in a temperature bath to achieve temperature upto 69 ^oC while stirring. The aqueous solution of ammonia (NH_3) as complexing agent was used. Aqueous NH_3 was used drop by drop in aqueous solution of $CdCl_2$ to dissolve precipitate of CdOH. The pH of the solution was stabilized at 11. Temperature of the solution of Thiourea was maintained at 69 ^oC in second temperature bath placed on digital hot plate. Aqueous solution of $(NH_2)_2CS$ was dropped slowly in aqueous solution of $CdCl_2$ at vigorous conditions of stirring. The temperature of the mixture was raised to 71±1 ^oC, rapidly. Cleaned substrates were dipped vertically in the solution with the help of self-made special holders. The container of solution was shielded to avoid the ammonia evaporation. Constant stirring was obtained using magnetic bar for the deposition time of 120 minutes. The constant stirring was necessary to ensure the homogeneous thickness of deposition at 71 ^oC±1 ^oC. Samples of thin films were taken out after 120 minutes of deposition time. All microscopic glass slide were washed ultrasonically in deionized water to eliminate loosely adhered particles of CdS. All samples were air dried in open atmosphere as in our previous paper [14]. One thin film sample from every solution concentration was air-annealed at a temperature 200 ^oC for 60 minutes. As-deposited thin film samples were marked as A_o [$CdCl_2$ (0.00312), $NH_2)_2CS$ (0.00625)], A_1 [$CdCl_2$ (0.000625, $NH_2)_2CS$ (0.00125)], A_2 [$CdCl_2$ (0.00125, $NH_2)_2CS$ (0.0025)], A_3 [$CdCl_2$ (0.0025, $NH_2)_2CS$ (0.005)] and A_4 [$CdCl_2$ (0.005, $NH_2)_2CS$ (0.01)]. Air annealed samples are marked as B_o [$CdCl_2$ (0.00312), $NH_2)_2CS$ (0.00625)], B_1 [CdCl2 (0.000625, $NH_2)_2CS$ (0.00125)], B_2 [$CdCl_2$ (0.00125, $NH_2)_2CS$ (0.0025)], B_3 [$CdCl_2$ (0.0025, $NH_2)_2CS$ (0.005)] and B_4 [$CdCl_2$ (0.005, $NH_2)_2CS$ (0.01)]. Ellipsometer was used to measure the thickness of the films. Radiation Cu K_α (λ = 1.540598 Å) was used for structural analysis using x-ray diffraction technique through (PANalytical X'Pert Pro PW1830). X'Pert High Score software were used to identify the crystalline phases of the films. Crystallite size (D) was calculated using the following Scherer formula;

$$D = \frac{0.94\,(\lambda)}{\beta\cos\theta} \tag{1}$$

where β is FWHM. Peaks of XRD were corrected for instrumental broadening. Theta (θ) is Bragg's angle, λ is the wavelength of the used x-ray, Scherrer constant (K=0.94) [16, 17, 24]. Optical transmittance (T) data was captured by double beam Photospectrometer (Shimadzu) for the wavelength range from 350 to 1100 nm. The absorption coefficient (α) was calculated by the following equation;

$$a = \frac{Ln(\frac{1}{T})}{d} \tag{2}$$

Using absorption coefficient (α), Optical energy band gap (E_g) was calculated by the equation;

$$a = \frac{A(h\upsilon - E_g)^n}{h\upsilon} \tag{3}$$

Here A is constant, photon energy ($h\upsilon$), n = 0.5 for direct allowed transitions because cadmium sulfide material is a direct band gap [18]. The parameters $(\alpha h\upsilon)^2$ are plotted as a function of photon energy ($h\upsilon$). The linear portion of the plotted curve was extrapolated to energy axis as

$(\alpha h\upsilon)^2 = 0$. This gives the value of E_g. Absorption coefficient (α) explains a tail for sub-band gap photon energy ($h\upsilon$). E_{oo} is the Urbach energy related with the width of tail and E_{oo} can be determined from the fit of the data [19];

$$a = a_o \, e^{h\upsilon/E_{oo}} \tag{4}$$

Here α_o is constant. The values of $Ln\alpha$ against the photon energy ($h\upsilon$) were plotted. The inverse of the slope from this graph gives the value of E_{oo}.

3. Results and discussion

XRD pattern of the thin films as-deposited and air-annealed show polycrystalline nature, Fig.1. The x-ray diffraction graphs have been scaled to a smaller size. Six graphs have been shown in one figure. Various small peaks have been lost in this presentation. All the peaks observed in these graphs are described in comprehensive detail.

All peaks of the sample A_o are cubic except the peak at $2\theta = 28.1544^o$ having plane (101) which belongs to the hexagonal phase (ref: 00-065-3414). The clear peaks for the sample B_o at $2\theta = 26.26.7070^o$, 44.2172^o, 52.4116^o belongs to (111), (220) and (311) planes of cubic CdS, respectively (ref: 01-080-0019). Very small peaks which cannot be seen in the given graph for this sample at $2\theta = 24.6780^o$, 28.384^o 58.4528^o, 66.698^o (ref: 00-001-0783) belongs to (100), (101), (202) and (203) belongs to hexagonal phase of CdS, respectively.

The clear peaks for sample A_1 at $2\theta = 26.7277^o$, 44.1346^o, 52.3619^o belongs to (111), (220), (311) cubic phase of CdS (ref: 01-080-0019), respectively. Three peaks at $2\theta = 26.1618^o$, 28.2306^o and 48.1229^o (ref: 01-080-0006) belongs to (100), (101), (103) hexagonal phase of CdS. Peaks for the sample B_1 at $2\theta = 26.8079^o$, 44.4133^o and 52.7364^o belongs to the (111), (220), (311) planes of the cubic CdS, respectively (ref: 01-075-0581). Four peaks at $2\theta = 26.9810^o$, 28.6450^o, 58.4937^o, and 66.7578^o (ref: 01-080-0006) belongs to (111), (101), (202), (203) hexagonal phase of CdS. This indicates the hexagonal phase is more prominent after heat treatment for this concentration of the solutions. A peak is also observed at $2\theta = 21.3924^o$ which belongs to monoclinic $CdSO_4$ (ref. 01-078-1874), [20, 21]. The peaks for the sample A_2 at $2\theta = 26.7405^o$, 44.2257^o, 52.3939^o and 54.9616^o can be related to the (111), (220), (311) and (222) planes of cubic CdS, respectively (ref: 01-075-0581). Only one peak at $2\theta = 28.1468^o$ belongs to plane (101) of hexagonal phase CdS, (ref: 01-072-2306). Peaks for the sample B_2 at $2\theta = 26.7670^o$, 44.4147^o, 52.4847^o are related to (111), (220), (311) planes of cubic CdS, respectively (ref: 01-080-0019). Three peaks only that are very small at $2\theta = 28.7526^o$, 58.4426^o, 66.6771^o, belongs to (101) hexagonal phase CdS (ref: 01-072-2306). This indicates the as-deposited films have very small peaks but three peaks after heat treatment are slightly clear. The peaks for the sample A_3 at $2\theta = 26.7247^o$, 44.2043^o, 52.4544^o and 55.0273^o belong to the (111), (220), (311) and (222) planes of cubic CdS, respectively (ref: 01-075-0581). Only one peak at $2\theta = 28.5542^o$ (ref: 00-001-0783) belongs to (101) hexagonal CdS. Peaks for the sample B_3 at $2\theta = 26.7520^o$, 44.5644^o (ref: 01-080-0006) are related to the (111), (220) cubic CdS, respectively. Only three very small peaks at $2\theta = 24.9624^o$, 26.6230^o, 28.5050^o, 48.2758^o, 58.9330^o, 67.0811^o, 73.2655^o (ref: 01-080-0006) belong to (111), (111), (101), (103), (202), (203), (114), hexagonal phase CdS, respectively. This indicates the as-deposited films have one very small peak but seven peaks after heat treatment are detected. This indicates that the heat treated samples have prominent hexagonal phase. Peaks for sample A_4 at $2\theta = 26.7552^o$, 30.3602^o, 44.2143^o, 52.3606^o, 55.0631^o are related to the (111), (200), (220), (311) and (222) planes of cubic CdS, respectively (ref: 01-080-0019). No peak related to hexagonal phase was detected. Peaks detected for B_4 at $2\theta = 26.7674^o$, 30.4024^o, 44.3195^o, 52.4880^o, 54.8619^o and 73.1410^o belong to (111), (200), (220), (311), (222) and (420) planes of cubic CdS, respectively (ref: 01-080-0006). No peak related to hexagonal phase was detected but peaks at $2\theta = 26.7674^o$, 52.4880^o, 54.8619^o may overlap with cubic phase that may not be distinguished separately. The XRD characterization propose that the hexagonal phase of CdS film developed prominently at the air-annealed samples for these solution concentrations [22]. The observations indicate that preferred orientation of the plane is (111).

Preferred orientation (111) is due to the nucleation controlled process that arises in the growing film. This proposes that the growth rate is slow in the film deposition process [23].

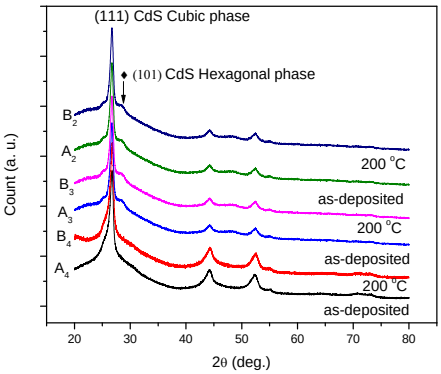

Fig. 1: XRD pattern of CdS film as-deposited and air-annealed

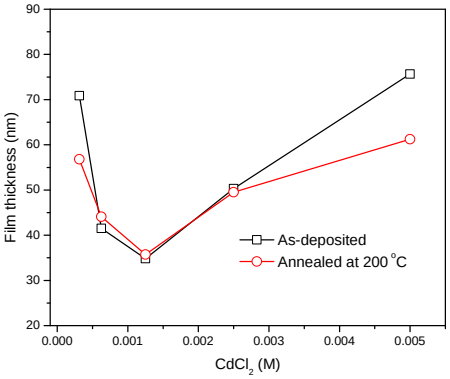

Fig. 2: Variation of film thickness with $CdCl_2$ concentration

The thickness of film samples as-deposited and air-annealed at the temperature 200 ^oC is discussed with the reference of $CdCl_2$ molar concentration. The film thickness is 70.8 nm at $CdCl_2$ concentration of 0.000312 M and is decreased to 42 nm at the $CdCl_2$ concentration of 0.00625 M of the as-deposited sample. The film thickness is minimum i.e. 34.8 nm for the 0.00125 molar concentration of $CdCl_2$ of the as-deposited sample as shown in fig. 2. Then the thickness is increased to 75.7 nm that is maximum value at the molar concentration 0.005 of $CdCl_2$ of the as-deposited sample.

This specifies that the thin film thickness has minimum value for the 0.00125 molar concentration of $CdCl_2$. The thickness of air-annealed film is 56.8 nm at molar concentration 0.000312 of $CdCl_2$. This thickness is less about 14 nm in comparison with the film thickness of as-deposited sample. Again the thickness of annealed film is less about 14.4 nm at the higher concentration of $CdCl_2$. The film thickness has the same values for the both as-deposited and annealed samples at the $CdCl_2$ molar concentration of 0.00625, 0.00125 and 0.0025 that is 42, 35 and 50 nm, respectively. This shows that the film thickness of the as-deposited and annealed for the ratio $CdCl_2$: $(NH_2)_2CS$ = 1:2 is the same specifically at the ratio [CdCl2 (0.000625, $(NH_2)_2CS$ (0.00125)], [$CdCl_2$ (0.00125, $(NH_2)_2CS$ (0.0025)] designated sample names as A_1 , A_2, A_3 and B_1 , B_2, B_3, respectively.

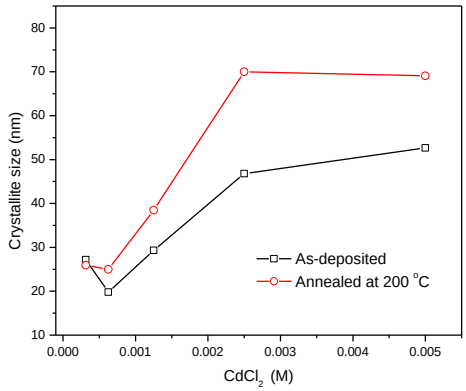

Fig. 3. Variation of crystallite size with $CdCl_2$

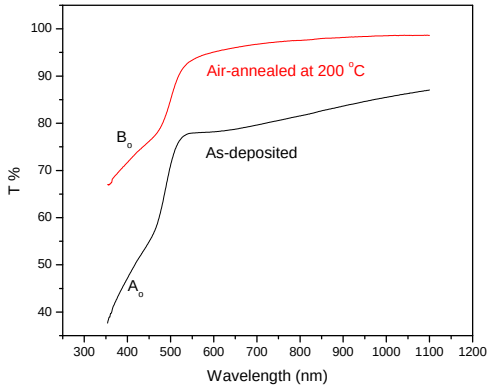

Fig. 4. Variation of T% on wavelength at low solution concentration

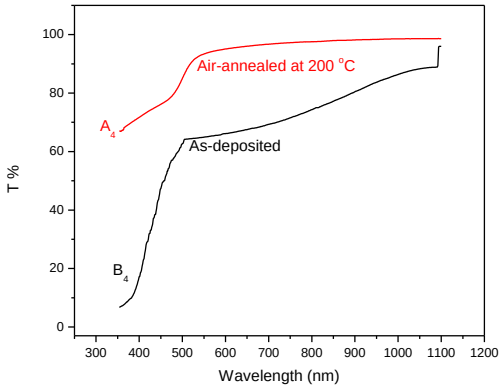

Fig. 5. Variation of T% on wavelength at higher solution concentration

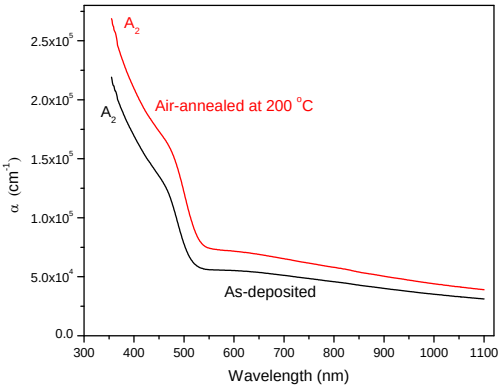

Fig. 6. Dependence of α on wavelength at lower solution concentration

Crystallite size (D) of the as-deposited thin film was 27.2 and 19.8 nm for concentration 0.000312, 0.000625 of $CdCl_2$, respectively fig. 3. It was increased to 52.6 nm when the concentration of $CdCl_2$ was increased for the as-deposited film samples. Crystallite size was 26 nm for the annealed film sample at the ratio $CdCl_2$:$(NH_2)_2CS$ = 0.000312:0.000625. The thickness is increased to about 70 nm with the increase of the molar concentration at the higher molar ratio. The crystallite size increases promently with increase of molar ratio. It is also very prominent difference in crystallite size for the as-deposited and air-annealed thin film samples.

Transmittance (T) spectra of CdS films of as-deposited and annealed film samples were recorded in the range of 350 nm-1100 nm. The transmittance (T) dependence of spectra on the molar concentration of solutions is discussed for both as-deposited and annealed film samples. Transmittance for the low solution concentration [$CdCl_2$ (0.00312 M), thiourea (0.00625 M)] was observed 78, 83, 86% at wavelengths 550, 850 and 1050 nm for the as-deposited samples, respectively. This Transmittance was increased to 93, 98 and 99% at the same wavelengths when samples were air-annealed at 200 ^oC as shown in fig. 4. No significant effect of annealing was observed for the solution concentration of [$CdCl_2$ (0.000625), $(NH_2)_2CS$ (0.00125)] and [$CdCl_2$ (0.00125), $(NH_2)_2CS$ (0.0025)]. Transmittance for the high solution concentration [$CdCl_2$ (0.005 M), Thiourea (0.01 M)] was observed 65, 72, 88% at wavelengths 550, 850 and 1050 nm for the as-deposited samples, respectively. This Transmittance was significantly increased to 94, 98 and 98% at the same wavelengths when samples were air-annealed at 200 ^oC as shown in fig. 5.

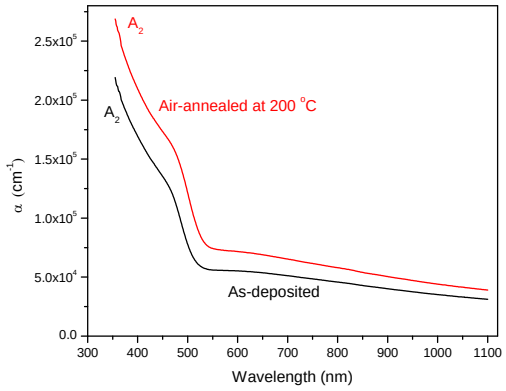

Fig. 7. Dependence of α on wavelength at higher solution concentration

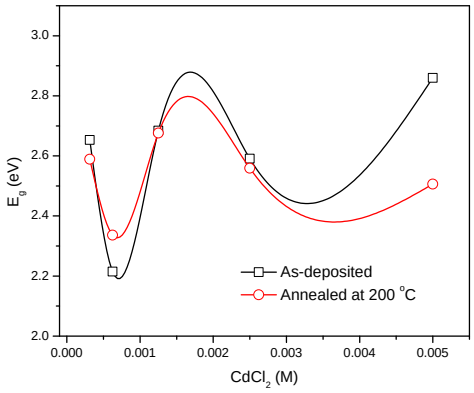

Fig. 8. Dependence of E_g on the concentration of $CdCl_2$

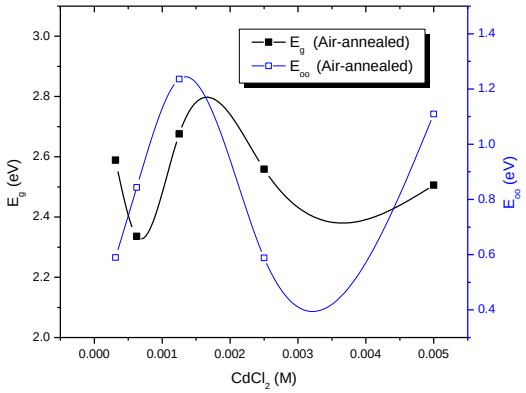

Fig. 9. Variation of E_g and E_{oo} with the concentration of $CdCl_2$

The dependence of α on the λ is shown in fig. 6 at the different concentrations of the solution. The value of α is increased with the annealing as shown in fig. 6. The value of α was increased with the increase of concentration of solution. It is also observed that the value of α was appreciably increased at all the wavelengths at the higher concentration of the solution fig. 7. E_g was calculated from the plot $(\alpha h\upsilon)^2$ against photon energy ($h\upsilon$) [23, 24]. The optical energy band gap is discussed here with reference to the solution concentration fig. 8. The value of E_g is 2.65 eV for the ratio $CdCl_2$:$(NH_2)_2CS$ = 0.000312:0.00625 of the as-deposited film and is slightly reduced to 2.59 eV for the air-annealed samples. E_g was decreased with the increase of solution concentration and again increased with the further increase of solution concentration. The value of the E_g is 2.59 eV and 2.56 eV for both the samples as-deposited and annealed samples at the concentration [$CdCl_2$ (0.0025, $(NH_2)_2CS$ (0.005)]. The E_g increased from 2.59 to 2.86 eV for the as-deposited sample with the increase of solution concentration from [$CdCl_2$ (0.0025 M, Thiourea (0.005)] to [$CdCl_2$ (0.005 M, Thiourea (0.01 M)]. No significant difference in the value of E_g was observed at higher solution concentration when the sample was air - annealed at 200 ^oC. Urbach energy (E_{oo}) is shown in for the annealed samples fig. 9. E_{oo} is also acknowledged as band tail width and this is because of the disorder in thin film sample material. The variation of bond angle and bond length from their standard values in crystalline material is known as disorder [25, 26, 27]. The optical band gap behavior is opposite to disorder. This behavior suggests that the observed optical energy band gap (E_g) is administrated with the variation of disorder in the film samples.

4. Conclusions

The CdS thin films were grown by CBD technique at different solution concentrations of CdS and $(NH_2)_2CS$. The bath temperature remained constant throughout the experiment. XRD characterization shows that all the grown films were in CdS cubic phase in as-deposited and few feeble peaks of hexagonal phase are present in all annealed film samples.

The crystallite size was increased with the increase of solution concentration. Also crystallite size enhanced with the annealing temperature. Optical band gap energy (E_g) was administrated with the phenomena of disordering. The optical Transmittance was varied with solution concentration and annealing temperature of the thin film samples.

Acknowledgement

This work is financially supported by the Higher Education Ministry of Malaysia and University Putra Malaysia through FRGS Project # 01-01-16-1835FR.

References

[1] Y. Chen, F. Wang, H. Xu, S. Ren, H. Gu, L. Wu, W. Wang, L. Feng, Chalcogenide Letters **14** (1), 1 (2017).
[2] S. Mokrushin, Y. Tkachev, Z. Kolloidn **23**, 438 (1961).
[3] G. Kitaev, A. Uritskaya, S. Mokrushin, Russ. J. Phys.Chem. **39**, 1101 (1965).
[4] Contreras, B. Egaas, K. Ramanathan, J. Hiltner, A.Swartzlander, F. Hasoon, R. Noufi, Prog. Photovolt, Res. Appl. **7**, 311 (1999).
[5] H. Khallif, I. O. Oladej, L. Chow, Thin Solid Films **516,** 5967 (2008).
[6] I. Oladeji, L. Chow, C. Ferekides, V. Viswanathan, Z. Zhao, Sol. Energy Mater. Sol. Cells **61,** 203 (2000).
[7] M. Contreras, M. Romero, B. To, F. Hasoon, R. Noufi, S. Ward, K. Ramanathan, Thin Solid Films **403/404**, 204 (2002).
[8] S. Vishnoi, R. Kumar, B. P. Singh, journal of intense pulsed lasers and applications in advanced physics **4** (1), 35 (2014).
[9] M. Becerril-Silva, O. Portillo-Moreno, R. Lozada-Morales, J. L. Fernandez-Muñoz, O. Zelaya-Ángel, Journal of Non-Oxide Glasses **9**(1), 1(2017).
[10] T. L. Chu, S. S. Chu, C. Ferekides, C. Q. Wu, J. Britt, C. Wang, J. Cryst. Growth **117**(1-4), 1073 (1992).
[11] C. Ferekides, J. Britt, Sol. Energy Mat. Sol. Cells **35**, 255 (1994).
[12] I. Kaur, D. K. Pandya, L. Chopra, J. Electrochem. Soc. **127**, 943 (1980).
[13] M. Froment, D. Lincot, Electrochim. Acta **40**, 1293 (1995).
[14] Z. Rizwan, A. Zakaria, M. G. M. Sabri, Fasih ud Din, Reza Zamiri, Monir Noroozi, M. Norizom, Chalcogenide Letters **7**(7), 471 (2010).
[15] Z. Rizwan, B. Z. Azmi, M. G. M. Sabri, Optoelectron. Adv. Mat. **5**(4), 393 (2011).
[16] S. Aghabeygi, Z. Sharifi , N. Molahasani, Digest Journal of Nanomaterials and Biostructures **12**(1), 81 (2017).
[17] M. Caglar, Y. Caglar, S. Ilican, J. Optoelectron. Adv. M. **8**(4), 1410 (2006).
[18] V. B. Sanap, B. H. Pawar Chalcogenide Letters **7**(3), 223 (2010)
[19] M. V. Kurik, Phys. Status Solidi. A **8**, 9 (1971).
[20] K. R. Murali Mary Mathelinea Rita Johnb Chalcogenide Letters **6**,(9) 483 (2009).
[21] S. Soundswarm, O. SenthilKumar, R. Dhanasekaran, Mater.Lett. **58**, 2381 (2004).
[22] G. C. Morris, R. Vanderveen, Sol. Energy Mater. Sol. Cells **27**, 305 (1992)
[23] G. Sasikala, P. Thilakan, C.Subramanian, Sol. Energ. Mat. & Sol. C., **62,** 275 (2000).
[24] E. G. Mornani, P. Mosayebian, D. Dorranian, K. Behzad, Journal of Ovonic Research **12**(2), 75 (2016).
[25] V. S. Sai Kumar, K. V. Rao, Journal of Optoelectronics and Biomedical Materials **9**(1), 27 (2017).
[26] Fangyang Liu, Yanqing Lai JunLiu, Bo Wang, Sanshuang Kuang, Zhian Zhang, Jie Li Yexiang Liu Journal of Alloys and Compounds **493**, 305 (2010).
[27] H. Moualkia, S. Hariech, M.S. Aida, Thin Solid Films **518**, 1259 (2009).